JCTC Journal of Chemical Theory and Computation

Article

pubs.acs.org/JCTC

Nuclear Velocity Perturbation Theory of Vibrational Circular Dichroism

A. Scherrer,[†,‡,§] R. Vuilleumier,*[,†,‡] and D. Sebastiani*[,§]

[†]UMR 8640 ENS-CNRS-UPMC, Département de Chimie, 24 rue Lhomond, École Normale Supérieure, 75005 Paris, France

[‡]UPMC Université Paris 06, 4, Place Jussieu, 75005 Paris, France

[§]Institute of Chemistry, Martin-Luther-Universität Halle-Wittenberg, von-Danckelmann-Platz 4, 06120 Halle (Saale), Germany

Supporting Information

ABSTRACT: We report the first implementation of vibrational circular dichroism (VCD) within density functional theory (DFT) using the nuclear velocity perturbation (NVP) theory. In order to support VCD calculations in large-scale systems such as solvated (bio)molecules and supramolecular assemblies, we have chosen a plane-wave electronic structure code (CPMD). This implementation allows the incorporation of fully anharmonic effects in VCD spectra on the basis of ab initio molecular dynamics simulations. On the conceptual level, we compare our NVP results for rigid molecules with an existing implementation based on the magnetic field perturbation (MFP) technique using a Gaussian basis set and find an excellent agreement. Regarding numerical aspects, we analyze our results for their correct origin dependence and gauge invariance of the physical observables. The correlation with experimental data is very satisfactory, with certain deviations mainly due to the level of electronic structure theory used.

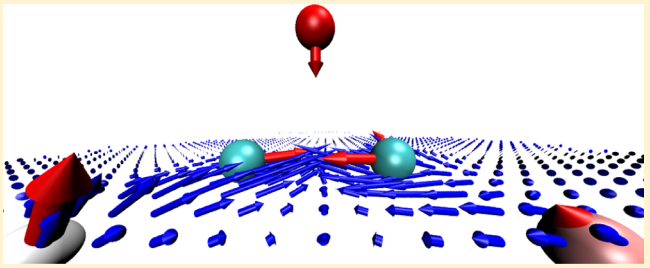

1. INTRODUCTION

Vibrational circular dichroism (VCD) describes the response of chiral molecules to left and right circularly polarized radiation in the infrared (IR) range. For enantiomers, the VCD spectrum shows the same intensities but has opposite signs. VCD spectroscopy is a widely used tool for the determination of the absolute configuration of chiral molecules.[1−4] Its application range comprises, in particular, most biomolecules (as, e.g., polypeptides). Because of its intrinsic connection to the underlying molecular structure, VCD is one of the most structurally sensitive spectroscopic techniques available.

The ab initio calculation of VCD has proven to successfully predict experimentally observable spectra.[3−5] Its presently most applied form is the magnetic field perturbation theory (MFP),[6] which is implemented in the Gaussian[7,8] and, e.g., more recently, in the ADF[9] packages.

An alternative theory of VCD was proposed theoretically by Nafie. He showed that the calculation of the required magnetic transition dipole moment needs non-Born−Oppenheimer contribution in the wave functions.[10,11] In the nuclear velocity perturbation theory (NVP),[12−14] this is achieved by the perturbative calculation of the complete adiabatic (CA) correction to the Born−Oppenheimer ground-state orbitals.[15−18] This provides a closely related yet conceptually different route for the calculation of VCD spectra. In particular, this allows for an efficient calculation of molecular dynamics-based VCD spectra. However, to this day, no successful implementation of the NVP-theory of VCD has been reported.[19]

It is known that the VCD spectrum is highly sensitive to configurational changes and solvation effects.[20−23] Theoretically, this has been addressed by incorporating anharmonicities and implicit or explicit solvant models.[24−26] However, the influence of hydrogen bonding solvents is known to require the consideration of explicit solvants beyond the harmonic approximation.[27] Furthermore, the increasing interest in VCD spectra for large-scale systems such as biomolecules has given rise to various fragmentation based approaches.[20,28−30] Both problems can naturally be addressed by our extension of the ab initio theory of VCD to extended systems.

In this work, we report the first implementation of the NVP theory of VCD. After revising the basic constituents of the harmonic VCD theory, we present a reformulation of Nafie's NVP theory within density functional theory (DFT)[31−33] using linear order density functional perturbation theory (DFPT).[34−39] The resulting expressions are implemented and numerically analyzed for their correct origin dependence and gauge invariance. The implementation is based on the plane-wave electronic structure code CPMD,[40] allowing for ab initio VCD calculations of extended systems such as solvated (bio)molecules and supramolecular assemblies. We compare our NVP results with an existing MFP implementation using Gaussian basis sets and find an excellent agreement of the harmonic spectra.

Received: August 7, 2013
Published: October 17, 2013

2. METHOD

2.1. Constituents of VCD Theory. The experimentally observable vibrational absorption intensities are theoretically accessible by the involved transition dipole moments. In the harmonic approximation, the dipole and rotational strengths for the $g_0 \rightarrow g_1$ vibrational transition in the electronic ground-state are given as

$$D_m^{(r)} = \mathrm{Re}[\langle \hat{\boldsymbol{\mu}} \rangle_m \cdot \langle \hat{\boldsymbol{\mu}} \rangle_m] \tag{1}$$

$$R_m^{(r)} = \mathrm{Im}[\langle \hat{\boldsymbol{\mu}} \rangle_m \cdot \langle \hat{\mathbf{m}} \rangle_m] \tag{2}$$

$$D_m^{(v)} = \mathrm{Re}[\langle \hat{\dot{\boldsymbol{\mu}}} \rangle_m \cdot \langle \hat{\boldsymbol{\mu}} \rangle_m] \omega_m^{-2} \tag{3}$$

$$R_m^{(v)} = \mathrm{Im}[\langle \hat{\dot{\boldsymbol{\mu}}} \rangle_m \cdot \langle \hat{\mathbf{m}} \rangle_m] \omega_m^{-1} \tag{4}$$

where (r) denotes the position and (v) the velocity form of the dipole and rotational strengths D and R, and the brackets $\langle \cdot \rangle$ represent the transition matrix element $g_0 \rightarrow g_1$ of the vibrational mode m with frequency ω_m. The electronic and magnetic dipole moments are composed of electronic and nuclear contributions:

$$\hat{\boldsymbol{\mu}} = \hat{\boldsymbol{\mu}}^e + \hat{\boldsymbol{\mu}}^n \tag{5}$$

$$= -\sum_j e\hat{\mathbf{r}}_j + \sum_\lambda eZ^\lambda \hat{\mathbf{R}}^\lambda \tag{6}$$

$$\hat{\mathbf{m}} = \hat{\mathbf{m}}^e + \hat{\mathbf{m}}^n \tag{7}$$

$$= -\sum_j \frac{e}{2c}\hat{\mathbf{r}}_j \times \hat{\dot{\mathbf{r}}}_j + \sum_\lambda \frac{eZ^\lambda}{2c}\hat{\mathbf{R}}^\lambda \times \hat{\dot{\mathbf{R}}}^\lambda \tag{8}$$

where the summation runs over all electronic states (j) and atoms (λ). In eqs 3 and 4, $\langle \hat{\dot{\boldsymbol{\mu}}} \rangle$ represents the total current,

$$\hat{\dot{\boldsymbol{\mu}}} = \hat{\dot{\boldsymbol{\mu}}}^e + \hat{\dot{\boldsymbol{\mu}}}^n \tag{9}$$

$$= -\sum_j e\hat{\dot{\mathbf{r}}}_j + \sum_\lambda eZ^\lambda \hat{\dot{\mathbf{R}}}^\lambda \tag{10}$$

and eq 3 corresponds to a current−current correlation. Equations 1−4 are valid in the absence of quadrupole contributions. This condition is fulfilled in the isotropic rotational ensemble average.[41] The meaning of the time derivatives $\hat{\dot{\mathbf{r}}}$ and $\hat{\dot{\mathbf{R}}}$, as well as derivations, with respect to $\dot{\mathbf{R}}$, will be clarified later.

The electronic and magnetic transition dipole moments arise due to the vibrational motion of the nuclei in the respective normal modes. They are related to the vibrational nuclear displacements via the total Atomic Polar Tensor $\mathcal{P}^\lambda$ (APT) and the Atomic Axial Tensor $\mathcal{M}^\lambda$ (AAT)

$$\mathcal{P}_{\alpha\beta}^\lambda = \mathcal{E}_{\alpha\beta}^\lambda + \mathcal{N}_{\alpha\beta}^\lambda \tag{11}$$

$$\mathcal{M}_{\alpha\beta}^\lambda = \mathcal{I}_{\alpha\beta}^\lambda + \mathcal{J}_{\alpha\beta}^\lambda \tag{12}$$

which have the following electronic (e) and nuclear (n) constituents:[19]

$$\mathcal{E}_{\alpha\beta}^{\lambda(r)} = \frac{\partial \langle \hat{\mu}_\beta^e \rangle}{\partial R_\alpha^\lambda} \tag{13}$$

$$\mathcal{E}_{\alpha\beta}^{\lambda(v)} = \frac{\partial \langle \hat{\dot{\mu}}_\beta^e \rangle}{\partial \dot{R}_\alpha^\lambda} \tag{14}$$

$$\mathcal{I}_{\alpha\beta}^\lambda = \frac{\partial \langle \hat{\dot{m}}_\beta^e \rangle}{\partial \dot{R}_\alpha^\lambda} \tag{15}$$

$$\mathcal{N}_{\alpha\beta}^{\lambda(r)} = \frac{\partial \langle \hat{\mu}_\beta^n \rangle}{\partial R_\alpha^\lambda} = eZ^\lambda \delta_{\alpha\beta} \tag{16}$$

$$\mathcal{N}_{\alpha\beta}^{\lambda(v)} = \frac{\partial \langle \hat{\dot{\mu}}_\beta^n \rangle}{\partial \dot{R}_\alpha^\lambda} = eZ^\lambda \delta_{\alpha\beta} \tag{17}$$

$$\mathcal{J}_{\alpha\beta}^\lambda = \frac{\partial \langle \hat{m}_\beta^n \rangle}{\partial \dot{R}_\alpha^\lambda} = \frac{eZ^\lambda}{2c} \sum_\gamma \varepsilon_{\alpha\beta\gamma} R_\gamma^\lambda \tag{18}$$

In the harmonic approximation, the expectation value for the nuclear contributions is taken classically which yields the analytical expressions given in eqs 16−18. The electronic contributions require a quantum mechanical expectation value that must be computed numerically. The involved dipole operators for the electronic degrees of freedom are

$$\hat{\boldsymbol{\mu}}^e = -e\hat{\mathbf{r}} \tag{19}$$

$$\hat{\dot{\boldsymbol{\mu}}}^e = -e\hat{\dot{\mathbf{r}}} \tag{20}$$

$$\hat{\mathbf{m}}^e = -\frac{e}{2c}\hat{\mathbf{r}} \times \hat{\dot{\mathbf{r}}} \tag{21}$$

where the velocity operator is

$$\hat{\dot{\mathbf{r}}} = \frac{i}{\hbar}[\hat{\mathbf{H}}^e, \hat{\mathbf{r}}] \tag{22}$$

Using Einstein's summation convention for repeated Greek indices, the dipole and rotational strengths of the mth normal mode in the position and the velocity form are

$$D_m^{(r)} = \mathcal{P}_{\alpha\beta}^{\lambda(r)} \mathcal{P}_{\alpha'\beta}^{\lambda'(r)} S_{\alpha m}^\lambda S_{\alpha' m}^{\lambda'} \tag{23}$$

$$R_m^{(r)} = \mathcal{P}_{\alpha\beta}^{\lambda(r)} \mathcal{M}_{\alpha'\beta}^{\lambda'} S_{\alpha m}^\lambda S_{\alpha' m}^{\lambda'} \tag{24}$$

$$D_m^{(v)} = \mathcal{P}_{\alpha\beta}^{\lambda(v)} \mathcal{P}_{\alpha'\beta}^{\lambda'(v)} S_{\alpha m}^\lambda S_{\alpha' m}^{\lambda'} \tag{25}$$

$$R_m^{(v)} = P_{\alpha\beta}^{\lambda(v)} \mathcal{M}_{\alpha'\beta}^{\lambda'} S_{\alpha m}^\lambda S_{\alpha' m}^{\lambda'} \tag{26}$$

The Cartesian displacement vector $\mathbf{S}_m^\lambda$ describes the displacement of nucleus λ in direction α due to the mth normal mode (Q_m):

$$S_{\alpha m}^\lambda = \left.\frac{\partial R_\alpha^\lambda}{\partial Q_m}\right|_{\mathbf{Q}=0} = \left.\frac{\partial \dot{R}_\alpha^\lambda}{\partial \dot{Q}_m}\right|_{\dot{\mathbf{Q}}=0} \tag{27}$$

2.2. Nuclear Velocity Perturbation in DFPT. By construction, the Born−Oppenheimer ground-state wave function does not contain the nuclear momentum information necessary for the calculation of electronic fluxes. This, in turn, is needed for the calculation of the magnetic transition dipole moment of a molecular system as required by the theory of VCD. In the literature, there are different perturbative approaches to address this problem, as outlined in the Introduction. In this work, the Nuclear Velocity Perturbation (NVP) approach, originally proposed theoretically by Nafie,[13]

is used. This requires the perturbative calculation of the complete adiabatic correction (CA) to the Born−Oppenheimer ground state. The following derivation of the NVP approach focuses on the implementation in the CPMD DFPT framework. For a detailed derivation, we refer the reader to the original theoretical works of Nafie or his recent book.[10,11,13,19]

The idea of the NVP approach is to take into account the linear term of the adiabatic coupling, which can be formulated in condensed form as

$$\langle\Psi_k|[\hat{T}^n, \Psi_k]\rangle = \langle\Psi_k|\hat{T}^n|\Psi_k\rangle + \langle\Psi_k|-i\hbar\partial_{\mathbf{R}}|\Psi_k\rangle\cdot\dot{\mathbf{R}} \tag{28}$$

where $\hat{T}^n$ is the nuclear kinetic energy operator, Ψ_k the total electronic wave function of state k. The linear term is taken as a perturbative correction to the electronic structure problem, i.e., a nuclear coordinate derivative is acting on the electronic degrees of freedom. This gives rise to an adiabatic imaginary correction to the Born−Oppenheimer ground-states, but leaves the electronic energy and, thus, the molecular dynamics unchanged. The resulting modified electronic structure problem is

$$(\mathcal{H}^e - E_k)|\Psi_k\rangle = i\hbar\dot{\mathbf{R}}\cdot\partial_{\mathbf{R}}|\Psi_k\rangle \tag{29}$$

which introduces a complex correction to the Born−Oppenheimer wave function. Separating real and imaginary part as adiabatic (A) and complete adiabatic (CA) contribution and developing to first order around $\boldsymbol{R}_0$ and $\dot{\mathbf{R}}_0 = 0$ gives the following Ansatz for the complex complete adiabatic wave function:

$$\tilde{\Psi}_k^{\mathrm{CA}}(\mathbf{r}, \mathbf{R}, \dot{\mathbf{R}}) = \Psi_k^{\mathrm{A}}(\mathbf{r}, \mathbf{R}) + i\Psi_k^{\mathrm{CA}}(\mathbf{r}, \mathbf{R}, \dot{\mathbf{R}}) \tag{30}$$

$$= \Psi_k^{\mathrm{A}}(\mathbf{r}, \mathbf{R}_0) + \Psi_k^{(\mathbf{R})}(\mathbf{r}, \mathbf{R}_0)\cdot(\mathbf{R} - \mathbf{R}_0) + i\Psi_k^{(\dot{\mathbf{R}})}(\mathbf{r}, \mathbf{R}_0, \dot{\mathbf{R}}_0)\cdot\dot{\mathbf{R}} \tag{31}$$

where the superscripts in parentheses, $(\mathbf{R})$ and $(\dot{\mathbf{R}})$, denote partial derivatives with respect to the corresponding quantity, e.g., $\Psi_k^{(\mathbf{R})} = \partial\Psi_k/\partial\mathbf{R}$. The real part of the adiabatic correction, i.e., the derivative with respect to a nuclear displacement $\mathbf{R}$, is accessible via DFPT calculation for a nuclear displacement perturbation.[38] As for the imaginary part, insertion of this Ansatz in eq 29 yields a Sternheimer-like equation, which can be solved iteratively:

$$(\mathcal{H}^e - E_k)\Psi_k^{(\dot{\mathbf{R}})} = \hbar\Psi_k^{(\mathbf{R})} \tag{32}$$

In the framework of single-determinant theories such as DFT and DFPT,[37,38] this relation directly translates to Kohn−Sham orbitals φ_o:

$$(\mathcal{H}_{\mathrm{KS}}^{(0)} - \varepsilon_o^{(0)})|\phi_o^{(\dot{\mathbf{R}})}\rangle = \hbar|\phi_o^{(\mathbf{R})}\rangle \tag{33}$$

Since $i\phi_o^{(\dot{\mathbf{R}})}$ is purely imaginary and does not change the electronic density, no self-consistent solution is required.

With this complete adiabatic correction (CA), it is possible to calculate the atomic tensors in the position and the velocity form. The electronic APT in the position and velocity form is

$$\mathcal{E}_{\alpha\beta}^{\lambda(r)} = \sum_o \mathcal{E}_{\alpha\beta}^{\lambda o(r)} = \sum_o \partial_{R_\alpha^\lambda}\langle\phi_o^{\mathrm{CA}}|\hat{\mu}_\beta^e|\phi_o^{\mathrm{CA}}\rangle = -2e\sum_o \langle\phi_o^{(0)}|\hat{r}_\beta|\phi_o^{(R_\alpha^\lambda)}\rangle \tag{34}$$

$$\mathcal{E}_{\alpha\beta}^{\lambda(v)} = \sum_o \mathcal{E}_{\alpha\beta}^{\lambda o(v)} = \sum_o \partial_{\dot{R}_\alpha^\lambda}\langle\phi_o^{\mathrm{CA}}|\hat{\mu}_\beta^e|\phi_o^{\mathrm{CA}}\rangle = -2e\sum_o \langle\phi_o^{(0)}|i\hat{r}_\beta|\phi_o^{(\dot{R}_\alpha^\lambda)}\rangle \tag{35}$$

and the electronic AAT is

$$\mathcal{I}_{\alpha\beta}^{\lambda} = \sum_o \mathcal{I}_{\alpha\beta}^{\lambda o} = \sum_o \partial_{\dot{R}_\alpha^\lambda}\langle\phi_o^{\mathrm{CA}}|\hat{m}_\beta^e|\phi_o^{\mathrm{CA}}\rangle = -\frac{ie}{c}\sum_{o\gamma\delta}\varepsilon_{\beta\gamma\delta}\langle\phi_o^{(0)}|\hat{r}_\gamma\hat{r}_\delta|\phi_o^{(\dot{R}_\alpha^\lambda)}\rangle \tag{36}$$

For both the APT in the velocity form and the AAT, the accuracy and the gauge invariance of the results highly depends on how well the hypervirial relation is satisfied:

$$\langle\phi_o^{\mathrm{CA}}|\hat{\boldsymbol{\mu}}|\phi_{o'}^{\mathrm{CA}}\rangle = \frac{i}{\hbar}\langle\phi_o^{\mathrm{CA}}|[\hat{\mathcal{H}}^e, \hat{\boldsymbol{\mu}}]|\phi_{o'}^{\mathrm{CA}}\rangle \tag{37}$$

This provides an important criterion for the basis set convergence. For a plane-wave basis with nonlocal pseudopotentials, this requires the explicit calculation of the commutator in the velocity operator in eq 22:[42]

$$\hat{\mathbf{r}} = \frac{i}{\hbar}[\hat{\mathcal{H}}^e, \hat{\mathbf{r}}] = \frac{-i\hbar}{m_e}\partial_{\mathbf{r}} + \frac{i}{\hbar}[\hat{V}_{\mathrm{nloc}}, \hat{\mathbf{r}}] \tag{38}$$

2.3. Gauge Dependencies. The APT shows no origin dependency whereas the exact AAT transforms under shifts of the gauge origin $O = O' + \Delta O = O' + \Delta$ as

$$\mathcal{M}_{\alpha\beta}^{\lambda O} = \mathcal{M}_{\alpha\beta}^{\lambda O'} - \frac{1}{2c}\varepsilon_{\beta\gamma\delta}\Delta_\gamma\mathcal{P}_{\alpha\delta}^{\lambda(v)} \tag{39}$$

In the common origin (CO) gauge, the rotational strength as a physical observable is gauge invariant:

$$R_m^{(r)} = \mathcal{P}_{\alpha\beta}^{\lambda(r)}\mathcal{M}_{\alpha'\beta}^{\lambda' O'}S_{\alpha m}^{\lambda}S_{\alpha' m}^{\lambda'} - \frac{1}{2c}\varepsilon_{\beta\gamma\delta}\Delta_\gamma\mathcal{P}_{\alpha\beta}^{\lambda(r)}\mathcal{P}_{\alpha'\delta}^{\lambda'(v)}S_{\alpha m}^{\lambda}S_{\alpha' m}^{\lambda'} \tag{40}$$

$$R_m^{(v)} = \mathcal{P}_{\alpha\beta}^{\lambda(v)}\mathcal{M}_{\alpha'\beta}^{\lambda' O'}S_{\alpha m}^{\lambda}S_{\alpha' m}^{\lambda'} - \frac{1}{2c}\varepsilon_{\beta\gamma\delta}\Delta_\gamma\mathcal{P}_{\alpha\beta}^{\lambda(v)}\mathcal{P}_{\alpha'\delta}^{\lambda'(v)}S_{\alpha m}^{\lambda}S_{\alpha' m}^{\lambda'} \tag{41}$$

since the second terms constitute triple products containing two identical vectors. For the position form of the rotational strength, this is only true if position and velocity forms of the APT are identical.

Alternatively, the distributed origin (DO) gauge provides different choices for the gauge, which helps to reduce the gauge dependence of the results introduced by basis set incompletion and discretization effects:

$$\mathcal{M}_{\alpha\beta}^{\lambda O} = (\mathcal{M}_{\alpha\beta}^{\lambda})_{\mathrm{DO}}^{\lambda} + \frac{1}{2c}\varepsilon_{\beta\gamma\delta}(R_\gamma^\lambda - O_\gamma)\mathcal{P}_{\alpha\delta}^{\lambda(v)} \tag{42}$$

In this nuclear DO gauge, each AAT is calculated with the nuclear position as the gauge origin. This reduces the magnitude of the position operator in eq 36 and thereby numerical instabilities.[43] The translation from the distributed origin to a common origin is achieved by the different

translation vectors and guarantees the required gauge invariance of the physical observable

$$R_m^{(v)} = \mathcal{P}_{\alpha\beta}^{\lambda(v)}(\mathcal{M}_{\alpha'\beta}^{\lambda'})_{\mathrm{DO}}^{\lambda'} S_{\alpha m}^{\lambda} S_{\alpha' m}^{\lambda'} + \frac{1}{2c}\varepsilon_{\beta\gamma\delta} R_\gamma^{\lambda'} \mathcal{P}_{\alpha\beta}^{\lambda(v)} \mathcal{P}_{\alpha'\delta}^{\lambda'(v)} S_{\alpha m}^{\lambda} S_{\alpha' m}^{\lambda'} \tag{43}$$

The overall expression is again invariant under translations of the origin. However, the last term cannot be factored out to form a triple product, because of the dependency of $R_\gamma^{\lambda'}$ on λ'. Therefore, the DO gauge is invariant under common translations of the origins but still requires the choice of a particular set of distributed origins.

Using eq 39, it is always possible to translate a DO gauge form of the AAT to a CO gauge form. In particular, it is also possible to define different sets of distributed origins. One convenient possibility is a set of statewise origins for the electronic AAT

$$\mathcal{I}_{\alpha\beta}^{\lambda O} = (\mathcal{I}_{\alpha\beta}^{\lambda})_{\mathrm{DO}}^{o} + \frac{1}{2c}\varepsilon_{\beta\gamma\delta}(\Delta_\gamma^o - O_\gamma)\mathcal{E}_{\alpha\delta}^{\lambda o(v)} \tag{44}$$

where $\mathcal{E}_{\alpha\delta}^{\lambda o(v)}$ is the contribution of the state o to the electronic APT in eq 35.

3. IMPLEMENTATION AND RESULTS

We have implemented the generalized Sternheimer equation (eq 33) in the CPMD code.[40] It is solved via an iterative conjugate gradient minimization and does not require a self-consistent solution. As for the related perturbation calculations, this approach does not involve a sum over excited states. Since the occurring perturbations do not include an explicit position operator, these calculations can be done using canonical orbitals ϕ_o. Because of the use of a plane-wave basis, no orbital-dependent gauge factors are required. This is a major advantage of this implementation, compared to atom-centered basis sets. As mentioned above, the use of nonlocal pseudo-potentials requires the explicit calculation of the commutator in eq 38. However, origin-dependent operators under periodic boundary conditions pose additional complications. Similar to the implementation for NMR,[44] the expectation values of the operators are taken with respect to maximally localized Wannier orbitals φ_o.[45] The perturbed canonical and localized states are mutually related via the same unitary transformation as that for the unperturbed ground-state orbitals.

$$|\varphi_o\rangle = \sum_{o'} U_{oo'}^{(0)} |\phi_{o'}\rangle \tag{45}$$

With this procedure, no cross terms between different Wannier orbitals arise.[44] This approach is based on the natural assumption that the response orbitals are sufficiently localized in the region of their respective unperturbed ground-state orbital. In the distributed origin gauge, the position operators are calculated with the corresponding Wannier center as its statewise origin:

$$\mathbf{r}_o = \langle\varphi_o|\hat{\mathbf{r}}|\varphi_o\rangle \tag{46}$$

We checked that the numerical results in a supercell calculation are the same for canonical and Wannier orbitals.

The established method to verify the accuracy of the numerical results is the comparison of the tensor sum rules for the APT and AAT.[43] They connect the magnetic property AAT with the electronic properties, i.e., the APT and the dipole moment. In particular, this allows to check for consistency of the implementation. In the notation of this work, the translational and rotational APT sum rules and the translational AAT sum rules are given as

$$\Sigma_{\alpha\beta}^0 = \sum_\lambda \mathcal{P}_{\alpha\beta}^{\lambda} \tag{47}$$

$$\Sigma_{\alpha\beta}^1 = \sum_\gamma \varepsilon_{\alpha\beta\gamma}\mu_\gamma^{\mathrm{G}} \tag{48}$$

$$\Sigma_{\alpha\beta}^2 = \sum_{\lambda\gamma\delta} \varepsilon_{\beta\gamma\delta} R_\gamma^{\lambda} \mathcal{P}_{\delta\alpha}^{\lambda} \tag{49}$$

$$\Sigma_{\alpha\beta}^3 = 2c\sum_\gamma \mathcal{M}_{\alpha\beta}^{\lambda} \tag{50}$$

where $\boldsymbol{\mu}^{\mathrm{G}}$ is the ground-state electric dipole moment. Σ^0 is zero for neutral systems and $\Sigma^1 = \Sigma^2 = \Sigma^3$ for all electron calculations in the basis set limit.

To benchmark the implementation, it is convenient to analyze small rigid molecules in the gas phase. We use R-d_2-oxirane for the different numerical benchmarks of the implementation (see Figure 1).

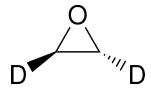

Figure 1. R-d_2-oxirane.

For the Σ^0 sum rule, which is ideally zero in all its components, we calculate the Frobenius norm $|\Sigma^0|$ to quantify the charge conservation. This provides a reference for the expected accuracy of the remaining sum rules. The dipole moment of R-d_2-oxirane lies along the C2 symmetry axis which is chosen to be the z-axis in our calculations. Therefore, only the xy- and the yx-components differ from zero and are opposite in sign and equal in magnitude. This is trivially fulfilled for Σ^1. The remaining APT and AAT sums are decomposed in their mean absolute value (symmetric) and the mean difference (antisymmetric); e.g., for Σ^2,

$$\overline{\Sigma_{xy}^2} = \frac{1}{2}||\Sigma_{xy}^2| + |\Sigma_{yx}^2|| \tag{51}$$

$$\Delta\Sigma_{xy}^2 = \frac{1}{2}||\Sigma_{xy}^2| - |\Sigma_{yx}^2|| \tag{52}$$

A proper benchmark of our implementation would require a separate comparison of NVP with MFP results on the one hand and the quantification of the effective core potential approximation (ECP) on the other hand. At present, however, this is not possible, since the MFP is not implemented in CPMD or plane-wave codes with comparable ECP. We choose the most commonly applied MFP implemented in the Gaussian package as a reference. Thereby, we directly compare our results to all electron (AE) ones. The basis set convergence for R-d_2-oxirane for different plane-wave energy cutoffs and the results for the MFP calculation with Gaussian basis sets are shown in Table 1.

The mean absolute values of the electronic sum rules converge with relative errors of the order of $|\Sigma^0|$, i.e., <1% for a plane-wave energy cutoff of 200 Ry. A suitable criterion for the required basis set convergence is the difference between the position and velocity form of the APT sum rules. Their relative

dx.doi.org/10.1021/ct400700c | J. Chem. Theory Comput. 2013, 9, 5305−5312

Table 1. Basis Set Convergence of the Sum Rules of the Atomic Tensors for R-d_2-Oxirane for the Effective Core Potential (ECP) Nuclear Velocity Perturbation (NVP) Implementation[a]

cutoff	$\lvert\Sigma^0\rvert$	Σ^1_{xy}	$\overline{\Sigma^{2(r)}_{xy}}$	$\Delta\Sigma^{2(r)}_{xy}$	$\overline{\Sigma^{2(v)}_{xy}}$	$\Delta\Sigma^{2(v)}_{xy}$	$\overline{\Sigma^{3}_{xy}}$	$\Delta\Sigma^{3}_{xy}$
050	0.0501	0.6700	0.6746	0.0058	0.7013	0.0066	0.6778	0.0911
100	0.0261	0.7577	0.7819	0.0039	0.7857	0.0040	0.7946	0.1095
150	0.0095	0.7570	0.7639	0.0040	0.7641	0.0040	0.7517	0.1005
200	0.0035	0.7572	0.7594	0.0003	0.7596	0.0004	0.7400	0.0921
250	0.0041	0.7571	0.7580	0.0008	0.7580	0.0008	0.7378	0.0935
AE MFP	0.0000	0.7547	0.7546	0.0000			0.7270	0.0037

[a]The all electron (AE) magnetic field perturbation (MFP) reference is calculated with the Gaussian 09 package. The atomic tensors are given in atomic units, and the plane-wave energy cutoff is given in Rydbergs. The computational details are appended as Supporting Information.

error is <1% already for a plane-wave energy cutoff of 100 Ry. Similarly, their mean differences is of the order 10^{-3} and reduces with increasing basis set completion. All electronic sum rules converge toward the MFP all-electron (AE) results with relative errors of $\sim 10^{-3}$ for 250 Ry.

The mean absolute values of the AAT translational sum rule $\overline{\Sigma^3_{xy}}$ shows parallel convergence to the electronic sum rules. Also here, the ECP results converge toward the AE results within a relative error of $\sim 10^{-2}$ for 250 Ry. Both the ECP NVP and the AE MFP results yield a systematically smaller AAT sum rule, with a relative deviation on the order of 10^{-2}, with respect to the electronic ones. However, the mean difference $\Delta\Sigma^3_{xy}$ shows a different behavior. For both, the ECP NVP and the AE MFP tensors, the difference $\Delta\Sigma^3_{xy}$ is larger than the electronic ones $\Delta\Sigma^{2(r)}_{xy}/\Delta\Sigma^{2(v)}_{xy}$. The ECP NVP difference is much larger than the AE MFP one and does not show any systematic dependence on the basis set. We attribute this shift of Σ^3_{xy} to the ECP approximation, since it does not show any gauge dependence. This is evident due to its symmetry, i.e., the equal sign of both entries, which differs from numerical errors introduced by basis set incompletion and the resulting gauge dependence which yields an antisymmetric contribution.

The calculation of magnetic properties such as the AAT requires the careful analysis of the gauge invariance of the resulting physical observables. This especially applies to the plane-wave basis with periodic boundary conditions. Even though the sum rules are not direct physical observables, they ideally are independent of the chosen origin and, hence, provide a handy way to check for the correct dependence of the intermediate results. Therefore, we compare the sum rules for distributed origin (DO) gauge calculations $(\Sigma)_{\mathrm{DO}}$ with common origin (CO) gauge calculations with different gauge origins $(\Sigma)^O_{\mathrm{CO}}$. For example, for the AAT sum rule, this reads as

$$(\Sigma^3)_{\mathrm{DO}} = 2c \sum_\lambda (\mathcal{M}^\lambda)^\lambda_{\mathrm{DO}} \tag{53}$$

$$(\Sigma^3)^O_{\mathrm{CO}} = 2c \sum_\lambda \mathcal{M}^{O\lambda} \tag{54}$$

Using the Frobenius norm, the relative error is

$$\varepsilon(\Sigma^3) = \frac{\lvert(\Sigma^3)^O_{\mathrm{CO}} - (\Sigma^3)_{\mathrm{DO}}\rvert}{\lvert(\Sigma^3)_{\mathrm{DO}}\rvert} \tag{55}$$

The gauge dependence of the sum rules for different distances of the R-d_2-oxirane molecule from the gauge origin is shown in Figure 2. The zero position corresponds to the molecular nuclear center of charge located at the origin of the position operator. We apply a sawtooth-shaped position operator for the

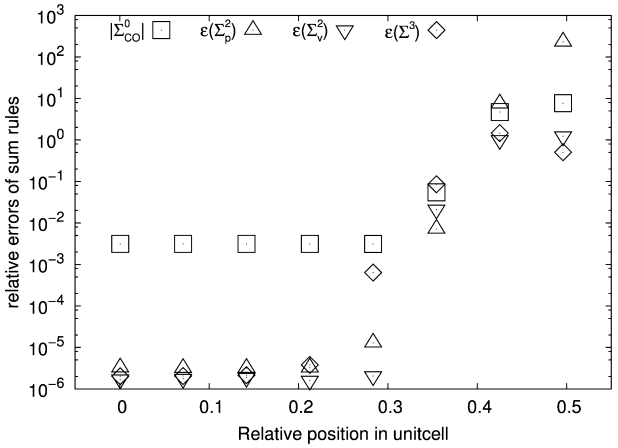

Figure 2. Relative errors of the atomic tensor sum rules using the common origin (CO) gauge and distributed origin (DO) gauge in the nuclear velocity perturbation (NVP). Dependence of the relative errors on the distance of the molecule to the box-centered gauge origin for a simulation supercell with a lattice size of 28 Å.

periodic boundaries that show a physically non-meaningful jump at the cell boundary (i.e., here at 0.5). The results for the CO and DO gauge calculations show a stable and gauge-independent behavior as long as the linear response orbitals do not extend to the ill-defined region of the jump in the position operator. For relative positions of the molecule from 0.0 to 0.25, the values are constant, indicating full gauge-invariance of our expressions. In particular, this allows for the translation of gauge origins in the distributed origin gauge. Note that the results in the distributed origin gauge are not affected by the jump of the sawtooth position operator. This holds as long as the orbitals are sufficiently localized in relation to the cell boundaries.

An interesting result is the different behavior of the position and velocity form of the APT. The velocity form does not show any systematic gauge dependence, not even on the logarithmic scale. The gauge dependence of the position form arises from numerical inaccuracies as, e.g., grid effects, which turn out to be of negligible absolute magnitude in our implementation (see Figure 2). This illustrates the potential of the NVP approach to obtain numerically gauge-invariant physical observables.

The calculation of isolated molecules using the supercell technique inherently introduces artificial interaction of the molecule with its periodic images. In particular, if the size of the supercell is insufficient, the molecule interacts with the dipole field of its mirror images. In order to quantify the relevance of this effect, we show the dependence of the sum rules on the cell

dx.doi.org/10.1021/ct400700c | J. Chem. Theory Comput. 2013, 9, 5305−5312

size in Figure 3. For all quantities, the decay perfectly follows the L^{-3} dipole contribution and, thus, can be controlled.

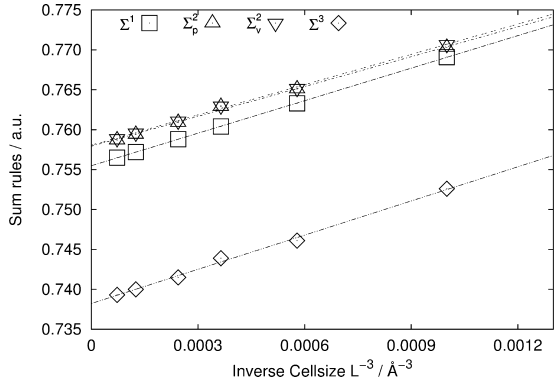

Figure 3. Dependence of the atomic tensor sum rules on the distance between the mirror images. The cell sizes are 10, 12, 14, 16, 20, and 24 Å.

Finally, the dipole- and rotational strengths as the desired physical observables must be benchmarked. Within the harmonic approximation, this requires the calculation of the normal modes at the respective equilibrium geometry. Again, we compare our ECP NVP results with the AE MFP results in the Gaussian framework. The dependence of the results on the similarity of the normal modes introduces another potential source of differences, which is known to be of the same order of magnitude as the inaccuracies of the actual atomic tensors.[46]

As benchmark systems, we again use R-d_2-oxirane, the closely related R-propylene-oxide (Figure 4), S-norcamphor (Figure 5), and R-α-pinene (Figure 6).

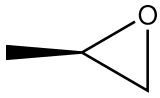

Figure 4. R-propylene-oxide.

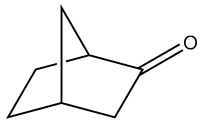

Figure 5. S-norcamphor.

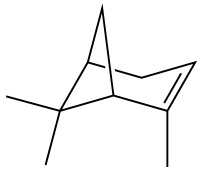

Figure 6. R-α-pinene.

The detailed table of the normal-mode frequencies and the dipole- and rotational strengths for R-d_2-oxirane is provided as Supporting Information. For visualization, we plot the correlation of the ECP NVP and the AE MFP results for the dipole- and rotational strengths in Figures 7−10).

The correlation with experimental data is very satisfactory, with virtually perfect agreement between our results (NVP) and the existing Gaussian-based implementation (MFP). There

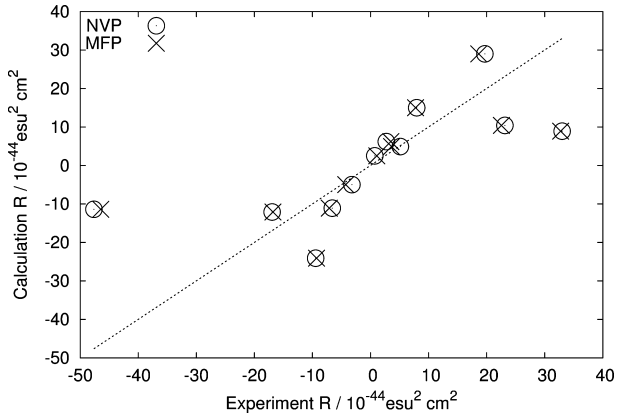

Figure 7. Correlation of experimental rotational strengths of R-d_2-oxirane with calculated ones using nuclear velocity perturbation (NVP) and magnetic field perturbation (MFP).

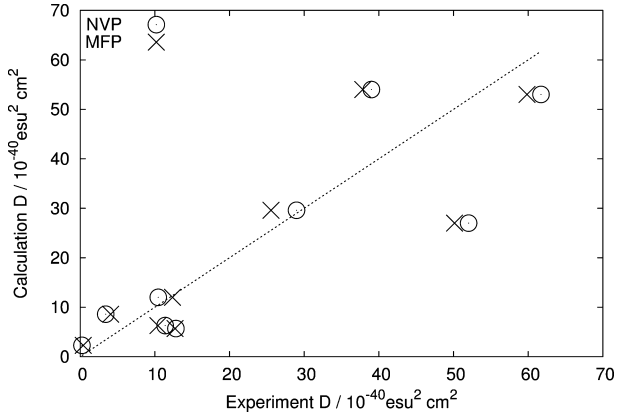

Figure 8. Correlation of experimental dipole strengths of R-d_2-oxirane with calculated ones using nuclear velocity perturbation (NVP) and magnetic field perturbation (MFP).

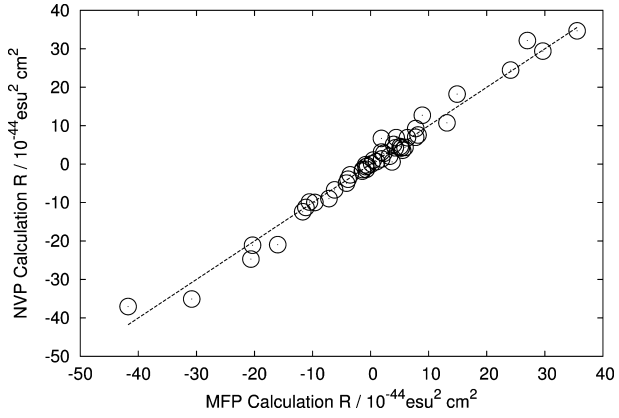

Figure 9. Correlation of rotational strengths of S-norcamphor calculated with magnetic field perturbation (MFP) and nuclear velocity perturbation (NVP).

are considerable numerical deviations of both methods with respect to the experiment, which have a variety of different reasons. Besides the level of theory (DFT, gradient-corrected xc-functional), the experimental values are mainly obtained in solution while the computed values represent gas-phase numbers. Here, the available experimental data for the enantiomer S-d_2-oxirane have been used.[47]

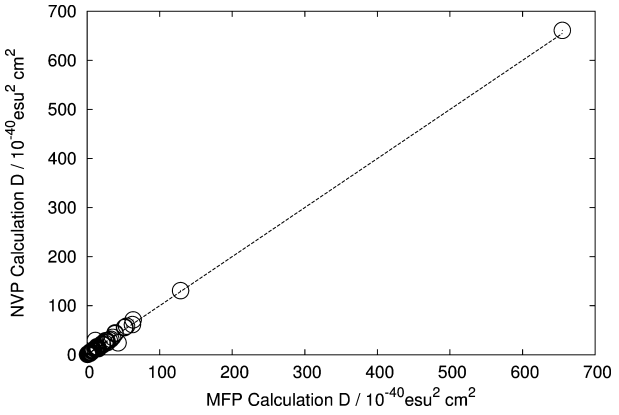

Figure 10. Correlation of dipole strengths of S-norcamphor calculated with magnetic field perturbation (MFP) and nuclear velocity perturbation (NVP).

In the bigger systems, such as α-pinene, the effect of mode degeneracies complicates the direct comparison. Some of the normal modes are degenerate and show a different symmetry, which strongly affects the sign of the individual contributions to the rotational strengths. However, this effect is a shortcoming of the harmonic analysis and not of the underlying atomic tensors. We have verified this qualitatively by taking the same normal modes for both calculations as is done for α-pinene (see the Supporting Information).

On the other hand, this subtle effect nicely illustrates the high sensitivity of VCD spectra on the molecular geometries, which represents one of the great strengths of this method and again highlights its suitability for structure determination.

4. CONCLUSION

We have presented the implementation of a reformulated nuclear velocity perturbation (NVP) theory of vibrational circular dichroism (VCD) within density functional perturbation theory (DFPT). Our results show the proper gauge invariance of the resulting physical observables. Our implementation in the plane-wave electronic structure code CPMD is the first successful NVP version of this theory. We have benchmarked our results against the popular magnetic field perturbation (MFP) theory implementation in the Gaussian 09 package and find them to be in remarkably good agreement. This work constitutes the basis for further application of ab initio calculation of VCD spectra for large biomolecular systems. In particular, NVP theory will allow for an efficient calculation of anharmonic VCD spectra based on ab initio molecular dynamics simulations.

■ ASSOCIATED CONTENT

Supporting Information

The Supporting Information gives additional data about computational details and MFP-NVP-correlation plots for the rotational strength and the dipole strength of R-propylene-oxide and R-α-pinene. This information is available free of charge via the Internet at http://pubs.acs.org.

■ AUTHOR INFORMATION

Corresponding Authors

*E-mail: rodolphe.vuilleumier@ens.fr.
*E-mail: daniel.sebastiani@chemie.uni-halle.de.

Notes

The authors declare no competing financial interest.

■ REFERENCES

(1) Nafie, L. A. *Annu. Rev. Phys. Chem.* **1997**, *48*, 357−386.
(2) Aamouche, A.; Devlin, F. J.; Stephens, P. J. *J. Am. Chem. Soc.* **2000**, *122*, 2346−2354.
(3) Freedman, T. B.; Cao, X.; Dukor, R. K.; Nafie, L. A. *Chirality* **2003**, *15*, 743−758.
(4) Magyarfalvi, G.; Tarczay, G.; Vass, E. *Wiley Interdiscip. Rev. Comput. Mol. Sci.* **2011**, *1*, 403−425.
(5) Stephens, P. J.; Devlin, F. J.; Pan, J.-J. *Chirality* **2008**, *20*, 643−663.
(6) Stephens, P. J. *J. Phys. Chem.* **1985**, *89*, 748−752.
(7) Cheeseman, J. R.; Frisch, M. J.; Devlin, F. J.; Stephens, P. J. *Chem. Phys. Lett.* **1996**, *252*, 211−220.
(8) Frisch, M. J.; Trucks, G. W.; Schlegel, H. B.; Scuseria, G. E.; Robb, M. A.; Cheeseman, J. R.; Scalmani, G.; Barone, V.; Mennucci, B.; Petersson, G. A.; Nakatsuji, H.; Caricato, M.; Li, X.; Hratchian, H. P.; Izmaylov, A. F.; Bloino, J.; Zheng, G.; Sonnenberg, J. L.; Hada, M.; Ehara, M.; Toyota, K.; Fukuda, R.; Hasegawa, J.; Ishida, M.; Nakajima, T.; Honda, Y.; Kitao, O.; Nakai, H.; Vreven, T.; Montgomery, J. A.,Jr.; Peralta, J. E.; Ogliaro, F.; Bearpark, M.; Heyd, J. J.; Brothers, E.; Kudin, K. N.; Staroverov, V. N.; Kobayashi, R.; Normand, J.; Raghavachari, K.; Rendell, A.; Burant, J. C.; Iyengar, S. S.; Tomasi, J.; Cossi, M.; Rega, N.; Millam, J. M.; Klene, M.; Knox, J. E.; Cross, J. B.; Bakken, V.; Adamo, C.; Jaramillo, J.; Gomperts, R.; Stratmann, R. E.; Yazyev, O.; Austin, A. J.; Cammi, R.; Pomelli, C.; Ochterski, J. W.; Martin, R. L.; Morokuma, K.; Zakrzewski, V. G.; Voth, G. A.; Salvador, P.; Dannenberg, J. J.; Dapprich, S.; Daniels, A. D.; Farkas, O.; Foresman, J. B.; Ortiz, J. V.; Cioslowski, J.; Fox, D. J.; *Gaussian 09, Revision A.02*, Gaussian, Inc.: Wallingford, CT, 2009.
(9) Nicu, V. P.; Neugebauer, J.; Wolff, S. K.; Baerends, E. J. *Theor. Chem. Acc.* **2007**, *119*, 245−263.
(10) Nafie, L. A.; Freedman, T. B. *J. Chem. Phys.* **1983**, *78*, 7108−7116.
(11) Nafie, L. A. *J. Chem. Phys.* **1983**, *79*, 4950−4957.
(12) Buckingham, A. D.; Fowler, P. W.; Galwas, P. A. *Chem. Phys.* **1987**, *112*, 1.
(13) Nafie, L. A. *J. Chem. Phys.* **1992**, *96*, 5687−5702.
(14) Nafie, L. A. *J. Phys. Chem. A* **2004**, *108*, 7222−7231.
(15) Freedman, T. B.; Shih, M.-L.; Lee, E.; Nafie, L. A. *J. Am. Chem. Soc.* **1997**, *119*, 10620−10626.
(16) Freedman, T. B.; Gao, X.; Shih, M.-L.; Nafie, L. A. *J. Phys. Chem. A* **1998**, *102*, 3352−3357.
(17) Abedi, A.; Maitra, N. T.; Gross, E. K. U. *Phys. Rev. Lett.* **2010**, *105*, 123002.
(18) Patchkovskii, S. *J. Chem. Phys.* **2012**, *137*, 084109.
(19) Nafie, L. A. *Vibrational Optical Activity: Principles and Applications*; Wiley−VCH: Chichester, U.K., 2011; pp 95−130.
(20) Bour, P.; Keiderling, T. A. *J. Phys. Chem. B* **2005**, *109*, 23687−23697.
(21) Kubelka, J.; Huang, R.; Keiderling, T. A. *J. Phys. Chem. B* **2005**, *109*, 8231−8243.
(22) Poopari, M. R.; Zhu, P.; Dezhahang, Z.; Xu, Y. *J. Chem. Phys.* **2012**, *137*, 194308.
(23) Longhi, G.; Abbate, S.; Lebon, F.; Castellucci, N.; Sabatino, P.; Tomasini, C. *J. Org. Chem.* **2012**, *77*, 6033−6042.
(24) Bak, K. L.; Bludský, O.; Jørgensen, P. *J. Chem. Phys.* **1995**, *103*, 10548−10555.
(25) Cappelli, C.; Bloino, J.; Lipparini, F.; Barone, V. *J. Phys. Chem. Lett.* **2012**, *3*, 1766−1773.
(26) Poopari, M. R.; Dezhahang, Z.; Yang, G.; Xu, Y. *ChemPhysChem* **2012**, *13*, 2310−2321.
(27) Polavarapu, P. L. *Chirality* **2012**, *24*, 909−920.
(28) Andrushchenko, V.; Tsankov, D.; Krasteva, M.; Wieser, H.; Bour, P. *J. Am. Chem. Soc.* **2011**, *133*, 15055−15064.
(29) Jiang, N.; Tan, R. X.; Ma, J. *J. Phys. Chem. B* **2011**, *115*, 2801−2813.

(30) Yamamoto, S.; Li, X.; Ruud, K.; Bour, P. *J. Chem. Theory Comput.* **2012**, *8*, 977−985.
(31) Hohenberg, P.; Kohn, W. *Phys. Rev.* **1964**, *136*, 864−871.
(32) Kohn, W.; Sham, L. J. *Phys. Rev.* **1965**, *140*, 1133−1138.
(33) Jones, R. O.; Gunnarsson, O. *Rev. Mod. Phys.* **1989**, *61*, 689−746.
(34) Gonze, X.; Vigneron, J.-P. *Phys. Rev. B* **1989**, *39*, 78112−13128.
(35) Giannozzi, P.; de Gironcoli, S.; Pavone, P.; Baroni, S. *Phys. Rev. B* **1991**, *43*, 7231−7242.
(36) Gonze, X.; Allan, D. C.; Teter, M. P. *Phys. Rev. Lett.* **1992**, *68*, 3603−3606.
(37) Gonze, X. *Phys. Rev. A* **1995**, *52*, 1096−1114.
(38) Putrino, A.; Sebastiani, D.; Parrinello, M. *J. Chem. Phys.* **2000**, *113*, 7102−7109.
(39) Baroni, S.; de Gironcoli, S.; dal Corso, A.; Giannozzi, P. *Rev. Mod. Phys.* **2001**, *73*, 515−562.
(40) *CPMD-3.15.3*, http://www.cpmd.org/ (accessed Aug. 1, 2013), Copyright IBM Corp., 1990−2008; Copyright MPI für Festkörperforschung Stuttgart, 1997−2001.
(41) Buckingham, A. D.; Dunn, M. B. *J. Chem. Soc.* **1971**, 1988.
(42) Pickard, C. J.; Mauri, F. *Phys. Rev. Lett.* **2003**, *91*, 196401.
(43) Stephens, P. J.; Jalkanen, K. J.; Amos, R. D.; Lazzeretti, P.; Zanasi, R. *J. Phys. Chem.* **1990**, *94*, 1811−1830.
(44) Sebastiani, D.; Parrinello, M. *J. Phys. Chem. A* **2001**, *105*, 1951−1958.
(45) Berghold, G.; Mundy, C. J.; Romero, A. H.; Hutter, J.; Parrinello, M. *Phys. Rev. B* **2000**, *61*, 1049611−1010048.
(46) Stephens, P. J.; Ashvar, C. S.; Devlin, F. J.; Cheeseman, J. R.; Frisch, M. J. *Mol. Phys.* **1996**, *89*, 579−594.
(47) Freedman, T. B.; Spencer, K. M.; Ragunathan, N.; Nafie, L. A.; Moore, J. A.; Schwab, J. M. *Can. J. Chem.* **1991**, *69*, 1619−1629.